Electronic confinement in the continuum: leaky Bragg mirror for electrons

Vitor Bento Sousa[1,5], Germano Maioli Penello[2,5], Pedro Henrique Pereira[1,3,5], Deborah Sivco[4], Claire Gmachl[4], Mauricio Pamplona Pires[2,5] and Patricia Lustoza Souza[1,5]

[1]LabSem/CETUC, Pontifical Catholic University of Rio de Janeiro, Rio de Janeiro, Brazil
[2]Physics Institute - Federal University of Rio de Janeiro, Brazil
[3]Institute of Ion Beam Physics and Materials Research, Helmholtz-Zentrum-Dresden-Rossendorf, Dresden, Germany
[4] Department of Electrical Engineering, Princeton University, Princeton, New Jersey, USA
[5]DISSE, Instituto Nacional de Ciência e Tecnologia de Nanodispositivos Semicondutores
e-mail: gpenello@if.ufrj.br

***Abstract*— In this work we present an InGaAs/InAlAs heterostructure lattice matched with InP that holds two leaky electronic states in the continuum. An optical analogy with Bragg mirrors is used to explain the origin and the desired characteristics of the leaky electronic state. Multipass waveguide absorption measurements were performed and theoretical calculations used to determine the energy levels involved in the optical transitions. The comparison between the theoretical and experimental oscillator strength shows the good optical quality of the sample.**

***Index Terms*— Quantum Well, Superlattice, Intersubband Transition, Leaky Electronic State in the Continuum, Photodetector.**

I. Introduction

A Photodetector is a device that absorbs light and generates photocurrent. Two different types of photodetectors exist based on its intrinsic ability to generate photocurrent. Thermal photodetectors absorb radiation and change their temperature which in turn changes other measurable physical property of the device [1]. Photon photodetectors are based on electronic transitions due to radiation absorption. After the absorption, the excited electron is collected and thus, generates photocurrent [2].

The energy levels and the intersubband transitions in a quantum well have been extensively studied to create photon photodetectors such as quantum well infrared photodetectors (QWIPs) [3]. The QWIP is a wavelength selective unipolar device in which the detection energy can be tuned by bandgap engineering.

The heterostructure of the detector is of paramount importance for designing a novel device. A quantum cascade detector (QCD) is an example of an innovative device that was developed by a detailed design of the band structure of the active region [4]. The heterostructure is designed in such a way that the electron absorbs light and generates photocurrent in a cascade of phonon emission.

Both QWIPs and QCDs depend on the electronic confinement and the energy levels that result from this confinement. In order to create another degree of freedom to tune the energy levels, photodetectors based on localized electronic states in the continuum were developed [5–9].

Recently, results on an asymmetric superlattice infrared photodetector were published detailing the concept of a leaky electronic state in the continuum and the photovoltaic effect - generation of photocurrent without external applied bias - obtained from transitions to the leaky electronic state. Because of the photovoltaic operation mode, this photodetector reached room temperature operation [10].

In this present work, we investigate the theoretical and experimental absorption spectra of an asymmetric superlattice with two leaky electronic states in the continuum. This heterostructure is idealized to produce a dual color infrared photodetector. The asymmetry of the heterostructure is designed in a way that each state in the continuum has a preferential direction for electron extraction. Electrons that are promoted to a higher energy level will flow to one direction while electrons that are promoted to a lower energy level will escape to the opposite direction.

II. Heterostructure Details

The heterostructure was simulated by using the split-operator method with position-dependent effective mass and nonparabolic approximations for the con-

Digital Object Identifier 10.29292/jics.v15i1.109

duction band [11, 12]. As a result, the energy levels and wavefunctions of each state were obtained and the theoretical absorption spectrum was calculated using the Fermi's golden rule by

$$\alpha(E) = \sum_n \frac{f_{1n}\Gamma}{2\pi\left[(E-E_n)^2 + \frac{1}{4}\Gamma^2\right]}. \quad (1)$$

In this equation Γ is the full width at half maximum (FWHM) of the Lorentzian distribution, E is the energy and E_n represents the energy of the n^{th} state. The f_{1n} is the oscillator strength of the optical transition between the ground state and the n^{th} state, given by:

$$f_{1n} = \frac{2m^*}{\hbar^2}(E_n - E_1)|\langle\psi_1|\hat{z}|\psi_n\rangle|^2, \quad (2)$$

where m^* is the effective mass, $\hbar$ is the reduced Planck constant, E_n and $|\psi_n\rangle$ are the energy and the states for the n^{th} level of the heterostructure, respectively.

In order to design the heterostructure, an optical analogy with Bragg mirrors was used. The leaky electronic states in the continuum are analyzed in a similar fashion of a leaky optical mode in an optical waveguide [13]. In our sample, a central quantum well is embedded in two different superlattices that can be thought of as Bragg mirrors for electrons. The superlattice in each side of the central quantum well "reflects" the wavefunction of different energy levels. This creates a leaky electronic state with an specific energy that is reflected due to the destructive interference of the wavefunction in one superlattice but not in the other. In other words, the state is "reflected" in one direction and extends to the opposite direction.

The simulated structure is an asymmetric $In_{0.53}Ga_{0.47}As/In_{0.52}Al_{0.48}As$ superlattice with a 2.5 nm thick central quantum well that separates two sections. In the left side of the central quantum there are five quantum wells (QWs) and five quantum barriers (QBs), with thicknesses of 2.0 nm and 3.5 nm, respectively. In the right side of the central quantum well there are also five QWs and five QBs with thicknesses of 2.0 nm and 7.0 nm. For these alloys, we use the conduction band offset of 502 meV [14].

The conduction band potential profile and the simulated electron probability density for the relevant states of the superlattice structure is shown in Fig. 1. The two states highlighted in the continuum are the first and the second leaky electronic states. In this simulation, one can clearly notice that the lowest leaky electronic state in the continuum (E = 566 meV) extends to the right but has no probability density on the left (painted in red color). The highest leaky electronic state in the continuum (E = 688 meV) extends to the left and has no probability density on the right (painted in blue color). The energy of the optical transitions for the first (red arrow) and second (blue arrow) leaky electronic states starting from the ground state are 308 meV and 430 meV, respectively. This is the expected behavior when compared to the optical Bragg mirror as explained above. Each superlattice acts as a Bragg mirror for electrons within an specific energy range. The miniband states below 500 meV are represented by gray lines. In principle, they are not involved in the optical transition because ideally only the ground state at 258 meV (painted in black color) is populated. The horizontal dashed line represents the calculated Fermi energy considering just the central quantum well *n*-doped with $2.0 \times 10^{18}\,\mathrm{cm}^{-3}$. At 80 K, the Fermi energy is localized 15 meV above the ground state.

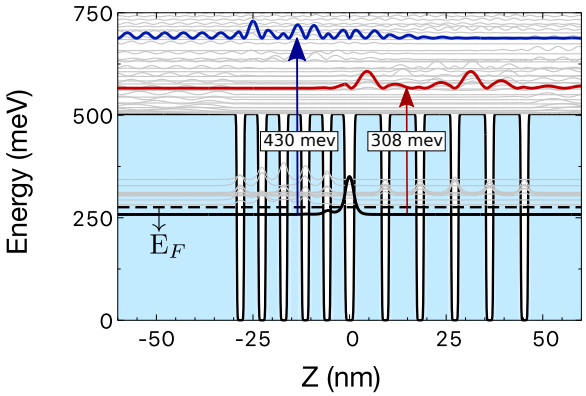

Fig. 1: Conduction band profile and electron probability density for the superlattice. The ground state and the two leaky electronic states in the continuum are represented by black, red and blue lines, respectively. The red and blue arrows represent the energy of the optical transition between the ground state and first and second leaky electronic states, respectively. The dotted line represents the Fermi energy at 78 K and it is localized 15 meV above the ground state.

III. Experimental Details

The superlattice structure based on $In_{0.53}Ga_{0.47}As$ and $In_{0.52}Al_{0.48}As$ is lattice matched to InP. In Fig. 1, the well is composed of InGaAs and the barrier of InAlAs. The sample was grown by molecular beam epitaxy (MBE). The active layer, detailed in the previous section, is repeated 20 times to increase absorption

and each repetition is separated with a 30 nm thick InAlAs barrier. To populate the ground state, the central QW was *n*-doped with a doping concentration of $2.0 \times 10^{18}\,\mathrm{cm}^{-3}$.

The absorption measurement was performed with a Fourier Transform Infrared Spectrometer (FTIR) in the 45 degree multipass waveguide geometry. The sample was mechanically lapped to obtain a mirror polished surface. At first, sandpaper was used for a rough surface leveling and then alumina spheres of 3.0 μm and 0.3 μm were used for the mirror polishing finish. The sample was mounted inside a cryostat with ZnSe windows and the sample temperature was controlled during the measurement.

IV. Results and Discussion

Fig. 2 shows the absorption spectra measured at 80 K, 200 K, and 300 K. Three peaks were obtained from this measurement, a low energy peak (around 250 meV), the main peak (310 meV) and a high energy peak (around 435 meV). The red and blue vertical lines symbolize the energy of the main and high energy peaks at 80 K. The main peak and the high energy peak, are attributed to the optical transitions between the ground state and the first and second excited states in the continuum, respectively. The low energy peak is attributed to transitions originating from the miniband states. The energies of the main and higher energy peaks are in good agreement with the optical transition energies seen in Fig. 1.

By analyzing the intensities of these energy peaks in Fig. 2, one notices that the lowest energy peak increases its intensity when compared to the main peak. This intensity increase with temperature shows that at low temperatures the miniband states were less populated, giving a lower intensity peak. As the temperature increases, the population of the miniband states also increases giving rise to the increase in the absorption of the lower energy peak. The high energy peak is smooth at 80 K and it is a shoulder-like for higher temperatures. A redshift in all peaks with increasing temperatures is observed, which is due to the temperature dependence of the bandgap of the alloys.

In order to compare the experimental absorption measurement with the calculated states in Fig. 1, we calculated the absorption spectrum using eq. 1 considering the ground state as the only populated state. A Lorentzian distribution with full width at half maximum (FWHM) of 10% of the peak energy was used for each transition. This value for the FWHM was chosen

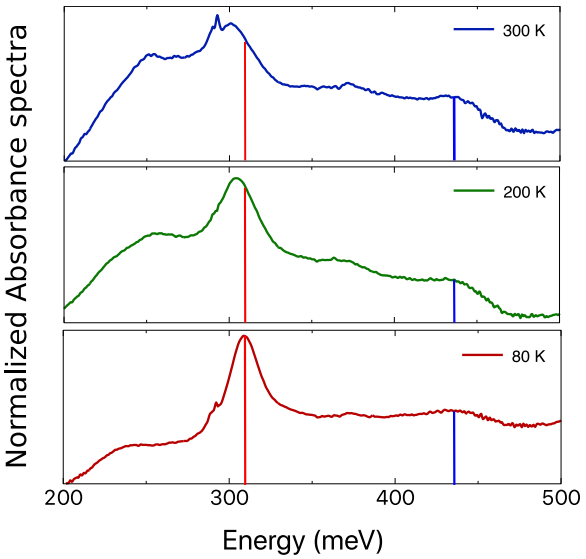

Fig. 2: Normalized Absorbance spectra measured at 80 K, 100 K and 300 K. Three distinguished peaks are observed. The main peak (around 310 meV) originates from transitions between the ground state and the first leaky electronic state. The high energy peak (around 435 meV) originates from transitions between the ground state and the second leaky electronic state. Transitions originating from the miniband states gives rise to the lowest energy peak (around 250 meV).

to simulate the broadening of a typical bound-to-bound transition in quantum wells.

Fig.3 shows an excellent agreement between the measurement and the simulated absorption spectrum for the main peak and a good agreement for the high energy peak. This is an experimental confirmation of the transitions between the ground states and the leaky states in the continuum. In this simulation, the ground state is the only populated state. Thus, transitions originating from the miniband are not obtained and the theoretical absorption spectrum does not show a peak around 250 meV.

The experimental oscillator strength (f) is determined through the area of the fitted Lorentzian for the main peak of the absorbance measurement, Fig. 2., by [2]:

$$\int_0^\infty \alpha(\nu)d\nu = \left(\frac{\rho_c N_w e^2 h f}{4\epsilon_0 m^* c n_r}\right)\left(\frac{\sin^2\theta}{\cos\theta}\right) \qquad (3)$$

where ρ_c is the 2D density of the electron in the quantum well, n_r is the index of refraction, N_w is the number of doped quantum wells and θ is the angle between direction of optical beam and the normal surface.

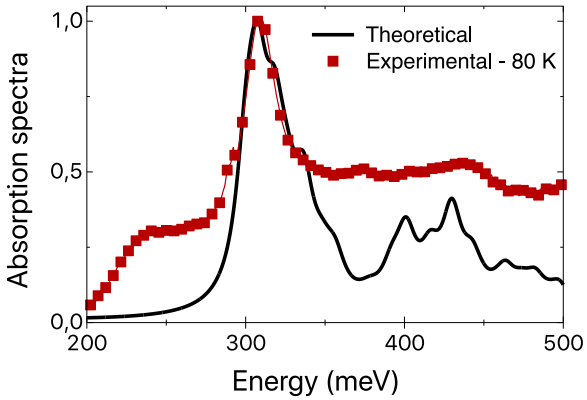

Fig. 3: Absorption spectrum at low temperature showing a good agreement between the experimental measurement and the theoretical calculation for the main (∼310 meV) and the high energy (∼435 meV) peaks. The theoretical modelling used only includes transitions originating from the ground state. The lowest energy peak (∼250 meV) in the experimental curve originates from the miniband states and are not calculated in the theoretical modelling.

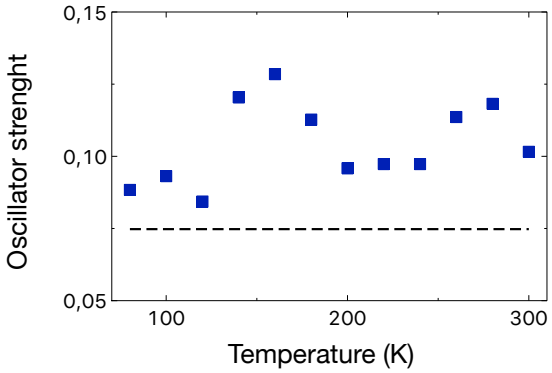

Fig. 4: Temperature dependence of the oscillator strength for the main peak transition. The blue squares represent the experimental result while the horizontal dashed line represents the theoretical value calculated.

The temperature dependence of the experimental oscillator strength (blue squares) and its theoretical value calculated using the eq. 2 (horizontal dashed line) are shown in Fig. 4. The amplitude of the uncertainty of each oscillator strength is smaller than the size of the square data. The experimental oscillator strength average was 0.099 ± 0.014 and its theoretical value is 0.075. This good agreement between them demonstrates a good optical quality of the sample.

V. Conclusion

In conclusion, we have shown an asymmetric superlattice structure that holds two leaky electronic states in the continuum. The design of the sample was based on an optical analogy with Bragg mirrors. The probability density of the leaky electronic states shows the expected behavior for each energy level. The electron is partially localized by a total reflection in one superlattice and a partial reflection in the other superlattice. The heterostructure was grown by MBE and absorption measurements were performed in a multipass waveguide geometry. The experimental absorption spectrum is in good agreement with the simulated optical transitions originating from the ground state. Transitions between the ground state and the first and the second electronic states are responsible for the main peak (around 300 meV) and the high energy peak (around 435 meV), respectively. The temperature dependence of the absorption spectra shows that transitions from the miniband are responsible for the lowest energy peak.

Our results show that the leaky electronic states have a good oscillator strength and could be used for a dual color infrared photodetector, where the leaky electronic state would generate current in opposite directions depending on the absorbed energy of the incident radiation. This will lead to a photodetector in which the sign of the measured current would distinguish the incoming radiation.

Acknowledgements

The authors would like to thank CAPES foundation, CNPq, FAPERJ, and FINEP for the financial support.

References

[1] P. Richards, "Bolometers for infrared and millimeter waves," *Journal of Applied Physics*, vol. 76, no. 1, pp. 1–24, 1994.

[2] B. Levine, "Quantum-well infrared photodetectors," *Journal of applied physics*, vol. 74, no. 8, pp. R1–R81, 1993.

[3] H. Schneider and H. C. Liu, "Quantum well infrared photodetectors," 2007.

[4] F. R. Giorgetta, E. Baumann, M. Graf, Q. Yang, C. Manz, K. Kohler, H. E. Beere, D. A. Ritchie, E. Linfield, A. G. Davies *et al.*, "Quantum cascade detectors," *IEEE Journal of Quantum Electronics*, vol. 45, no. 8, pp. 1039–1052, 2009.

[5] R. Leavitt and J. Little, "Infrared photodetector based on intersubband transitions to minigap-confined states in doped quantum wells," *Applied Physics Letters*, vol. 79, no. 13, pp. 2091–2093, 2001.

[6] G. M. Penello, M. H. Degani, M. Z. Maialle, R. M. Kawabata, D. N. Micha, M. P. Pires, and P. L. Souza, "Exploring parity anomaly for dual peak infrared photodetection," *IEEE Journal of Quantum Electronics*, vol. 52, no. 12, pp. 1–6, 2016.

[7] L. Guerra, G. Penello, M. Pires, L. Pinto, R. Jakomin, R. Mourão, M. Degani, M. Maialle, and P. Souza, "Detecting infrared radiation beyond the bandoffset with intersubband transitions," *IEEE Photonics Technology Letters*, vol. 28, no. 15, pp. 1641–1644, 2016.

[8] P. H. Pereira, G. M. Penello, M. P. Pires, D. Sivco, C. Gmachl, and P. L. Souza, "High performance dual-mode operation asymmetric superlattice infrared photodetector using leaky electronic states," *Journal of Applied Physics*, vol. 125, no. 20, p. 204501, 2019.

[9] G. M. Penello, P. H. Pereira, L. Guerra, L. D. Pinto, R. Jakomin, R. T. Mourão, M. H. Degani, M. Z. Maialle, D. Sivco, C. Gmachl *et al.*, "Progress in symmetric and asymmetric superlattice quantum well infrared photodetectors," *Annalen der Physik*, vol. 531, no. 6, p. 1800462, 2019.

[10] G. M. Penello, P. H. Pereira, M. P. Pires, D. Sivco, C. Gmachl, and P. L. Souza, "Leaky electronic states for photovoltaic photodetectors based on asymmetric superlattices," *Applied Physics Letters*, vol. 112, no. 3, p. 033503, 2018.

[11] M. H. Degani and M. Z. Maialle, "Numerical calculations of the quantum states in semiconductor nanostructures," *Journal of Computational and Theoretical Nanoscience*, vol. 7, no. 2, pp. 454–473, 2010.

[12] K. Yoo, L. Ram-Mohan, and D. Nelson, "Effect of nonparabolicity in gaas/ga 1- x al x as semiconductor quantum wells," *Physical Review B*, vol. 39, no. 17, p. 12808, 1989.

[13] P. T. Kristensen, C. Van Vlack, and S. Hughes, "Generalized effective mode volume for leaky optical cavities," *Optics letters*, vol. 37, no. 10, pp. 1649–1651, 2012.

[14] I. Vurgaftman, J. á. Meyer, and L. á. Ram-Mohan, "Band parameters for iii–v compound semiconductors and their alloys," *Journal of applied physics*, vol. 89, no. 11, pp. 5815–5875, 2001.